Dynamic Modeling of Pressure Reducing Valves

Simon L. Prescott[1] and Bogumil Ulanicki[2]

Abstract: Models are currently available for representing the dynamical behavior of most water network components. Such models are relatively simple, accurate and can be easily solved. However, there is no generally accepted dynamic model of a pressure reducing valve (PRV). The key contributions of this paper are the development of several dynamic models—two phenomenological, one behavioral, and one linear—to represent the behavior of PRVs. The models vary in complexity but perform similarly. Experimental data is used to assess the accuracy of the models. The phenomenological models are derived from physical laws and provide an excellent but complex representation of a PRV. The behavioral model is simpler and sufficient for most practical purposes. The linear model does not take the needle valve setting (which controls the valve's speed) into account and therefore has limited use.

DOI: 10.1061/(ASCE)0733-9429(2003)129:10(804)

CE Database subject headings: Dynamic models; Hydraulic networks; Valves; Water pressure.

Introduction

Water utilities use pressure control to reduce background leakage and the incidence of pipe bursts. Control is usually implemented across areas that are typically supplied through pressure reducing valves (PRVs) and closed at all other boundaries. Single-feed PRV schemes are often adopted for ease of control and monitoring but risk supply interruption in the event of failure. Multifeed systems improve the security of supply but are more complex and incur the risk of PRV interaction leading to instability. A better understanding of the dynamics of PRVs and networks will lead to improved control strategies and reduce both instabilities and leakage.

Dynamic modeling allows for an investigation of certain aspects of network behavior (e.g., sustained oscillation or fast pressure surges) that cannot be identified through steady state modeling. Network dynamics are described by a system of differential algebraic equations (DAEs) or, in the case of transients, partial differential algebraic equations (PDAEs). Routines to solve PDAEs have been available for some time (Brenan et al. 1996) but are often complex and lack robustness. For this reason, it is desirable to keep models simple.

There is a large amount of work involving both PRVs and their solution in steady state models (Jeppson 1976; Anderson and Powell 1999; Khezzar et al. 1999; Simpson 1999). The effect of automatic control valves on transient dynamics has been investigated (Brunone and Morelli 1999) and general methods to incorporate modulating valves into transient simulation software have been discussed (McInnis et al. 1997). Both papers use a standard valve model with an opening that is adjusted at a constant rate.

In this paper, four dynamic PRV models are presented. A detailed phenomenological model is constructed from applying physical laws to the individual elements that make up a PRV. This model is accurate but complex so its solution in large networks is difficult. However, it provides a basis for simpler models and gives a reference from which to judge their accuracy. Another model is formed by introducing simplifying assumptions in the detailed phenomenological model and therefore retains its major features but is easier to simulate. A behavioral model, formed from observations of the PRV on a test rig, is also presented. This is the simplest model, easiest to solve and sufficiently accurate in normal operating conditions. A linear model has also been developed by linearizing the detailed phenomenological model about its steady state but this model is independent of the needle valve setting.

Physical experiments have been performed on a test rig to aid the construction of the models and to assess their validity. The tests can be split into two groups—the first experiments investigate the static characteristics of the individual elements that make up a PRV while the second establish the dynamic behavior of the whole PRV. The purpose of a PRV is to maintain a fixed outlet pressure (set point) by adjusting its opening.

A typical PRV has a structure similar to that of Fig. 1—a main valve is operated by a control loop consisting of a fixed orifice, a pilot valve, and a needle valve connecting the loop to the control space (chamber above the main valve). The valve shown is a Cla-val NGE9001 but the models developed here can be easily adapted to any PRV.

If the outlet pressure is higher than required, the pilot valve will close causing an increase in T-junction pressure. This will cause some of the pilot loop flow to enter the control space via the needle valve. The control space pressure will therefore increase causing the main valve to close. This will reduce the outlet pressure, as required. Similarly, if the outlet pressure is too low, the pilot valve will open, T-junction pressure will drop, and the control space will begin to empty. This will cause the main valve to open and the outlet pressure to increase. The needle valve restricts flow and therefore the speed at which the PRV can open and close. On the Cla-val, the user can set the rate of PRV opening.

[1]Research Fellow, Water Software Systems, De Montfort Univ., Queens Building, The Gateway, Leicester, LE1 9BH, UK. E-mail: slp@dmu.ac.uk

[2]Director of Research, Water Software Systems, De Montfort Univ., Queens Building, The Gateway, Leicester, LE1 9BH, UK. E-mail: bul@dmu.ac.uk

Note. Discussion open until March 1, 2004. Separate discussions must be submitted for individual papers. To extend the closing date by one month, a written request must be filed with the ASCE Managing Editor. The manuscript for this paper was submitted for review and possible publication on September 7, 2001; approved on February 21, 2003. This paper is part of the ***Journal of Hydraulic Engineering***, Vol. 129, No. 10, October 1, 2003. ©ASCE, ISSN 0733-9429/2003/10-804–812/$18.00.

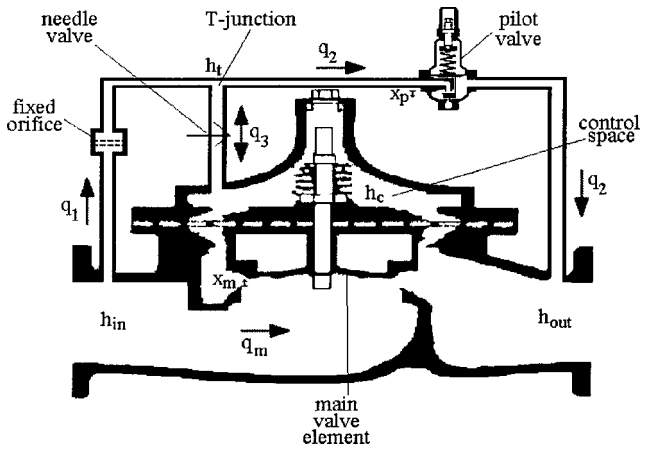

Fig. 1. Cla-val pressure reducing valve (reproduced with permission)

If the inlet pressure is too low to maintain the required outlet pressure, the PRV will open fully and act like a short pipe. If the outlet pressure is higher than the inlet, the PRV completely closes to prevent reverse flow. The performance of a PRV in both these scenarios has been previously studied (Khezzar et al. 1999; Simpson 1999), so the analysis in this paper will be restricted to active operation where the main valve adjusts to maintain the desired outlet pressure.

Dynamic Pressure Reducing Valve Models

All PRV models form a system of DAEs which can be solved using standard methods (Brenan et al. 1996). The ease and speed of solution depends on the size of the network in which the PRV is modeled, the type of pipe model (rigid-column, transient, etc.), and the choice of PRV model.

Full Phenomenological Model

The only moving parts of the PRV are the main and pilot valve elements (see Fig. 1). The motion of each valve element is described by a second order differential equation, given in Eq. (1) for the main valve and Eq. (2) for the pilot valve.

$$m_m\ddot{x}_m=\rho g(h_{\text{in}}a_1+h_{\text{out}}(a_2-a_1)-h_c a_2)-m_m g-f_m\dot{x}_m+\frac{\rho q_m^2}{a_1} \tag{1}$$

$$m_p\ddot{x}_p=k_{\text{spr}}(p_{\text{sp}}-x_p)-\rho g h_{\text{out}}a_d+m_p g-f_p\dot{x}_p \tag{2}$$

The subscripts, m and p refer to the main and pilot valves, respectively, and x = displacement of the valve from its closed position [m]; m = mass of the valve [kg]; f = friction constant opposing the motion of the valve [N/(m/s)]; $h_{\text{in}}, h_{\text{out}}, h_c, h_t$ = inlet, outlet, control space, and T-junction pressures [m]; a_1, a_2 = areas of the bottom and top of the main valve [m^2]; a_d = area of the pilot valve diaphragm [m^2]; q_m = main valve flow [m^3/s]; k_{spr} = pilot valve spring constant [N/m]; ρ = density of water [kg/m^3]; and g = acceleration due to gravity [m/s^2]. The force terms of Eq. (1) are, from left to right, inlet pressure acting on the base of the main valve, outlet pressure acting on the region of the diaphragm around the top of the main valve, control space pressure acting on the other side of this diaphragm, weight of the main valve, friction acting on the main valve, and force caused by change of momentum of water as its velocity goes to zero as it hits the base of the main valve. The force terms of Eq. (2) are, from left to right, the spring acting on the pilot valve diaphragm, outlet pressure acting on the other side of this diaphragm, the weight of the pilot valve, and friction opposing its motion.

The other variable in Eq. (2) is p_{sp} which represents the PRV set point and is physically given by a combination of pilot screw position and spring length. The force exerted by the pilot spring is $k_{\text{spr}}(p_{\text{sp}}-x_p)$ and increasing p_{sp} corresponds to tightening the spring with the pilot screw, thus increasing set point.

There are six algebraic equations to represent flows through the control loop and main valve. The flow through the fixed orifice, needle valve, pilot valve, and main valve are given by equations of the form $q=C_v\sqrt{|\Delta h|}\,\text{sgn}(\Delta h)$ where q = flow through the element, Δh = pressure loss across the element, and C_v = valve capacity of the element. The valve capacity is the flow per root of pressure loss and is expressed as a function of opening. The valve capacity is usually given in the manufacturers' literature for the main valve and can be obtained experimentally for the others.

The two equations given in Eq. (3) complete the algebraic part of the model. These are the continuity of flow at the T-junction and a relationship between the needle valve flow and main valve velocity.

$$q_1+q_3=q_2,\quad q_3=f(x_m)\dot{x}_m \tag{3}$$

where q_1, q_2, q_3 = flow through the fixed orifice, pilot valve, and needle valve, respectively. As the main valve opens or closes, the volume of water in the control space changes at a rate equivalent to the flow through the needle valve. For piston operated PRVs, the area of the top of the main valve remains constant over the entire stroke so the function $f(x_m)$ is constant. The PRV under consideration in this paper is diaphragm operated so the area of the top of the main valve element changes with the opening of the valve. The full model can now be written

$$m_m\ddot{x}_m=\rho g(h_{\text{in}}a_1+h_{\text{out}}(a_2-a_1)-h_c a_2)-m_m g-f_m\dot{x}_m+\frac{\rho q_m^2}{a_1}$$

$$m_p\ddot{x}_p=k_{\text{spr}}(p_{\text{sp}}-x_p)-\rho g h_{\text{out}}a_d+m_p g-f_p\dot{x}_p$$

$$q_3=f(x_m)\dot{x}_m$$

$$q_m=C_{\text{vm}}(x_m)\sqrt{|h_{\text{in}}-h_{\text{out}}|}\,\text{sgn}(h_{\text{in}}-h_{\text{out}})$$

$$q_1=C_{\text{vfo}}\sqrt{|h_{\text{in}}-h_t|}\,\text{sgn}(h_{\text{in}}-h_t)$$

$$q_2=C_{\text{vp}}(x_p)\sqrt{|h_t-h_{\text{out}}|}\,\text{sgn}(h_t-h_{\text{out}})$$

$$q_3=C_{\text{vnv}}\sqrt{|h_c-h_t|}\,\text{sgn}(h_c-h_t)$$

$$q_1+q_3=q_2 \tag{4}$$

where a_2 = function of x_m, C_{vm}, and C_{vp} = valve capacities of the main valve and pilot valve, respectively, and C_{vfo} and C_{vnv} = constants representing the capacity of the fixed orifice and needle valve. Although the needle valve is adjustable, its setting does not normally change during PRV operation and so a constant suffices.

Simplified Phenomenological Model

DAE solvers can simulate the full model in a small network but do not always converge when more complex networks need to be solved. It is useful to look for simplifications which ease computation and yet preserve the main structure of the model.

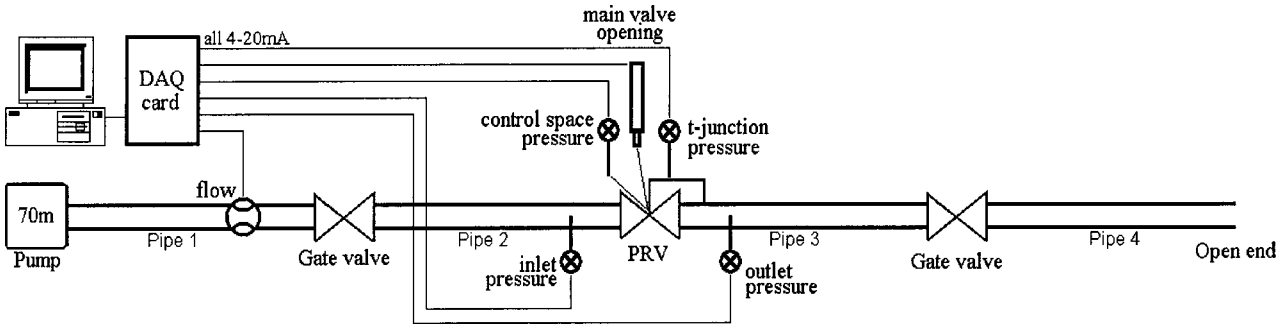

Fig. 2. System layout

Normally, the flow through the main valve, pilot valve, and fixed orifice will be in one direction so the signum part can be omitted as well as the absolute values. The flow through the needle valve travels in both directions so it is necessary to include the full equation in the model. From modeling experience, the friction and inertia terms in Eqs. (1) and (2) are negligible when compared with the pressure terms and the term involving the pilot spring. Simulation of the full model in Eq. (4) and its simplified version—Eq. (5)—give indistinguishable results. The simplified model is

$$\dot{x}_m = \frac{1}{f(x_m)} q_3$$

$$\rho g(h_{\text{in}} a_1 + h_{\text{out}}(a_2 - a_1) - h_c a_2) - m_m g + \frac{\rho q_m^2}{a_1} = 0$$

$$k_{\text{spr}}(p_{\text{sp}} - x_p) - \rho g h_{\text{out}} a_d + m_p g = 0$$

$$q_m = C_{\text{vm}}(x_m)\sqrt{h_{\text{in}} - h_{\text{out}}}$$

$$q_1 = C_{\text{vfo}}\sqrt{h_{\text{in}} - h_t}$$

$$q_2 = C_{\text{vp}}(x_p)\sqrt{h_t - h_{\text{out}}}$$

$$q_3 = C_{\text{vnv}}\sqrt{|h_c - h_t|}\,\text{sgn}(h_c - h_t)$$

$$q_1 + q_3 = q_2 \tag{5}$$

This model has just one differential equation that links the motion of the main valve to flow through the needle valve. All other equations from the detailed model are preserved in a simpler algebraic form.

Behavioral Model

In this section, another model is described which is significantly simpler than the phenomenological models but behaves similarly in normal operating conditions. The model was formulated by observing the behavior of the PRV in the test rig and of the full model during a change of either the set point or the surrounding network. From observations, the main valve opening follows an exponential curve. To generate such behavior, the derivative of x_m should be proportional to the difference between a given set point h_{set}, and the current outlet pressure h_{out}. To preserve the relationship between relating flow and pressure drop, the main valve characteristic is maintained.

$$\dot{x}_m = \begin{cases} \alpha_{\text{open}}(h_{\text{set}} - h_{\text{out}}), & \dot{x}_m \geq 0 \\ \alpha_{\text{close}}(h_{\text{set}} - h_{\text{out}}), & \dot{x}_m < 0 \end{cases}$$

$$q_m = C_{\text{vm}}(x_m)\sqrt{h_{\text{in}} - h_{\text{out}}} \tag{6}$$

There are two values of α depending on whether the PRV is opening (α_{open}) or closing (α_{close}). In the phenomenological models (and in reality) the desired outlet pressure is given by the setting of the pilot screw and changes slightly as the system changes. In the behavioral model, a value is given for the desired outlet pressure and this will be the actual outlet pressure following changes to the system. Since the role of the PRV is to maintain a fixed outlet pressure, it is acceptable to fix the set point in this way. The only unknown parameters in the behavioral model are α_{open} and α_{close}, which should be obtained from an identification experiment.

Linear Model

Linear models are convenient to explicitly understand system dynamics and to derive control strategies. Such a model is obtained by linearizing the differential part of the system about a steady state. A PRV cannot be linearized in isolation from the network since inlet and outlet pressure depend on the system in which the PRV is installed. The system model can be represented by

$$\dot{\mathbf{x}} = \mathbf{f}(\mathbf{x},\mathbf{y},\mathbf{u}), \quad \mathbf{g}(\mathbf{x},\mathbf{y},\mathbf{u}) = \mathbf{0} \tag{7}$$

where x = vector of differential variables, y = vector of algebraic variables; and u = vector of control inputs (set point, inlet pressure to system, etc.). A steady state $(\mathbf{x}_s, \mathbf{y}_s, \mathbf{u}_s)$ is given by setting $\mathbf{f}(\mathbf{x},\mathbf{y},\mathbf{u}) = \mathbf{0}$ in Eq. (7). Using a first order Taylor series to expand Eq. (7) about the steady state and solving for $\delta\dot{x}$

$$\delta\dot{\mathbf{x}} \approx \mathbf{A}\delta\mathbf{x} + \mathbf{B}\delta\mathbf{u} \tag{8}$$

where $\mathbf{A} = (\mathbf{f}_x - \mathbf{f}_y\mathbf{g}_y^{-1}\mathbf{g}_x)$, $\mathbf{B} = (\mathbf{f}_u - \mathbf{f}_y\mathbf{g}_y^{-1}\mathbf{g}_u)$, and $\mathbf{f}_x, \mathbf{f}_y, \mathbf{f}_u, \mathbf{g}_x, \mathbf{g}_y, \mathbf{g}_u$ = matrices formed by differentiating $\mathbf{f}$ and $\mathbf{g}$ by $\mathbf{x}$, $\mathbf{y}$ and $\mathbf{u}$, evaluated at $(\mathbf{x}_s, \mathbf{y}_s, \mathbf{u}_s)$. The matrices $\mathbf{A}$ and $\mathbf{B}$ are used to evolve the vector $\mathbf{x}$ from steady state, following a change in $\mathbf{u}$.

This method has been used to construct a linear model of a PRV in a simple two pipe network (Prescott and Ulanicki 2001). In the linear model the setting of the needle valve had no effect. This is because at steady state, there is no flow through the needle valve and therefore its setting plays no part in the linear model. The linear model was observed to behave in a similar way to the full model with the needle valve fully open.

Physical Measurements

All measurements were performed on the same PRV using the same computer monitoring system, shown in Fig. 2. The available transducers were two magnetic flow meters, one linear variable differential transformer (LVDT), four pressure transducers, and a differential pressure cell. The static characteristics of the control

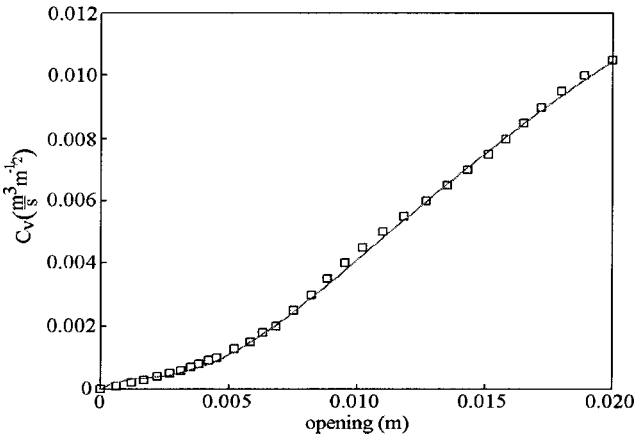

Fig. 3. Main valve capacity

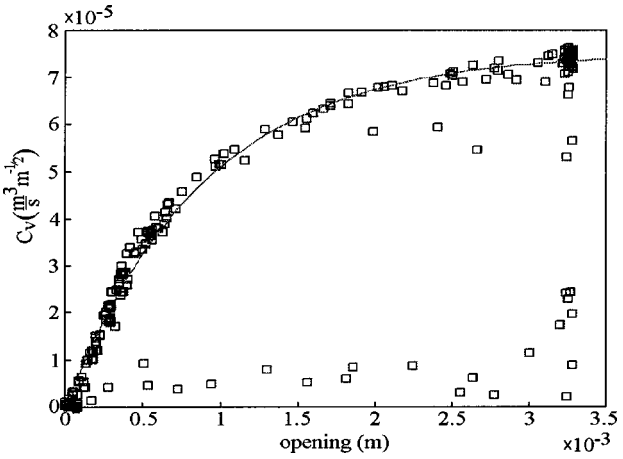

Fig. 4. Pilot valve capacity characteristic

loop elements were determined using the differential pressure cell, a flow meter, and the LVDT if necessary. The observed quantities during experiments on the PRV in the test system were inlet, outlet, T-junction, and control space pressure, main valve flow, and opening of the PRV. Measurements were recorded at 0.25 s intervals.

Parameters and Characteristics

The parameters of the PRV can either be obtained from the manufacturer or measured. In this case, the given parameters are $m_m = 8$ kg, $a_1 = 0.0078$ m^2, $a_2 = 0.0218$ m^2, and the measured ones are $a_d = 0.00196$ m^2, $m_p = 0.1$ kg, $k_{spr} = 70{,}000$ N/m. The static characteristics of the control loop elements have been individually determined by experiment.

Main Valve Capacity

The main valve capacity was measured by observing the pressure drop across and flow through the main valve for a range of openings. The shape of the characteristic lends itself to being approximated by exponential functions so, using the Levenberg-Marquardt method (Press et al. 1992) to fit a function consisting of four exponential curves, the PRV main valve capacity in the model is given by

$$C_{vm}(x_m) = 0.02107 - 0.02962e^{-51.1322x_m} + 0.0109e^{-261x_m} - 0.00325e^{-683.17x_m} + 0.0009e^{-399.5x_m} \quad (9)$$

Note that the curve satisfies $C_{vm}(0) = 0$. This curve is shown in Fig. 3 (solid line) with the manufacturers data (dots).

Pilot Valve Capacity

The pilot valve capacity was established by the same procedure as the capacity of the main valve and is shown in Fig. 4. Most of the points lie on a curve given by

$$C_{vp}(x_p) = 0.0000753(1 - e^{-1135x_p}) \quad (10)$$

which is also shown as a solid line in Fig. 4. A few points do not lie in the vicinity of the line where oscillation of the pilot valve occurred during the experiments but the static characteristic can still be easily identified.

Fixed Orifice

The area of the fixed orifice remains constant so the relationship between pressure drop and flow is quadratic as shown in Fig. 5. A straight line fitted to this data has slope 0.00003, the capacity of the fixed orifice. According to standard theory (Streeter et al. 1998), orifice flow is given by

$$q = ca\sqrt{2g\Delta h} \quad (11)$$

where c = discharge coefficient and a = area of the orifice. The area of the fixed orifice has been measured as 7.92×10^{-6} m^2 so the valve capacity translates as a discharge coefficient c of 0.855. Theoretically, values of c of around 0.8 correspond to a cylindrical orifice.

Needle Valve

The needle valve opening is adjustable for flow in one direction only (in this case from the control space to the T-junction) and is usually set during PRV installation. As before, the pressure loss across the needle valve and the flow through it are measured. This is performed over a range of needle valve settings and for different flow directions.

Fig. 6, corresponding to main valve opening, shows the pressure/flow relationship for several needle valve settings. The flow increases linearly with the root of the pressure drop and then saturates. Since the saturation occurs at a relatively large pressure drop, an equation similar to that for the fixed orifice is expected to be sufficient. The equation for the flow through the needle valve

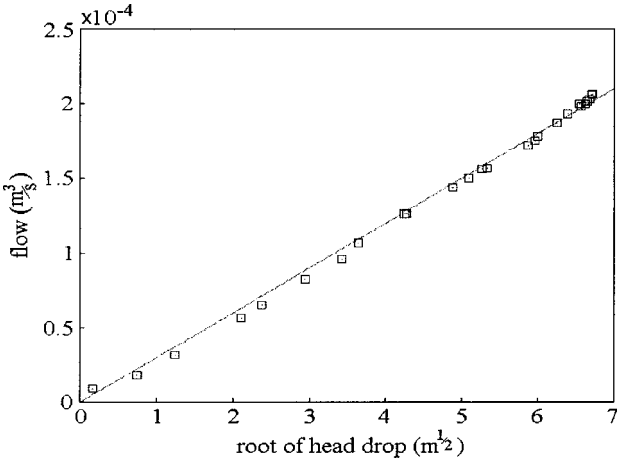

Fig. 5. Fixed orifice characteristic

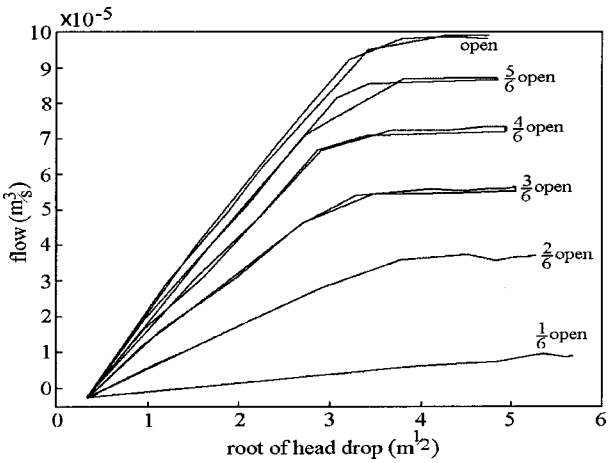

Fig. 6. Needle valve characteristic (flow out of control space)

is given by $q_3 = C_{\text{vnv}}\sqrt{h_c - h_t}$. The value of the constant C_{vnv} is determined by the needle valve setting.

The points in Fig. 7 show the same variables but for flow going into the control space. The needle valve setting has no effect on the characteristic although there is a little hysteresis probably due to the needle valve spring. This is assumed to be negligible so a straight line, also shown in Fig. 7, is used. The resulting equation for the needle valve during main valve closure is $q_3 = 0.00011\sqrt{h_t - h_c}$ which represents a discharge coefficient of $c = 0.8$ since the area of the needle valve is 31.17×10^{-6} m^2 for flow in this direction.

Control Space

To establish the relationship between the needle valve flow and the velocity of the main valve, the control space volume was determined experimentally for various main valve openings. The opening of the main valve in relation to the volume of water ejected from the control space is shown in Fig. 8. The data points initially follow a smooth curve then deviate from it at larger openings, likely to be caused by the diaphragm ''rolling.'' For selecting a PRV, the manufacturer suggests a maximum opening of 70% (marked in Fig. 8) in normal operation. Based on this, an exponential curve, given in Eq. (12), is used to model the control space volume.

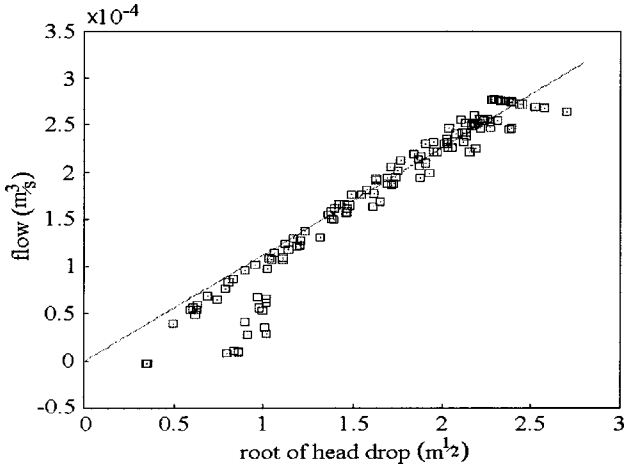

Fig. 7. Needle valve characteristic (flow into control space)

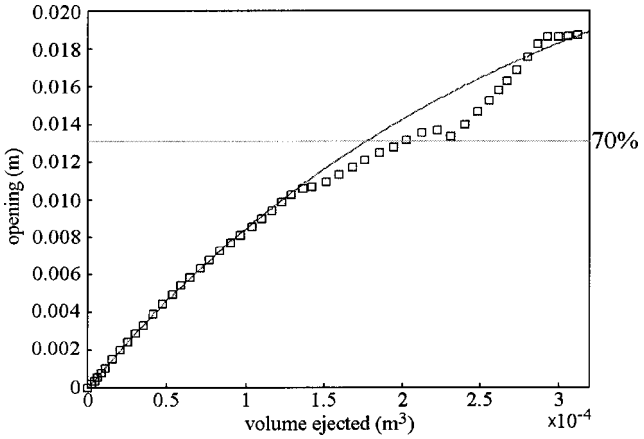

Fig. 8. Control space volume

$$x_m = 0.02732(1 - e^{-3700V}) \tag{12}$$

Differentiating this, an expression relating the flow through the needle valve and velocity of the main valve can be obtained (using $q_3 = \dot{V}$)

$$\dot{x}_m = 3700(0.02732 - x_m)q_3 \tag{13}$$

which is used in the phenomenological models. For the diaphragm valve, the total area at the bottom of the control space a_2 can be determined by rearranging Eq. (12) to obtain an expression for V and then differentiating with respect to x_m. The resulting area is

$$a_2 = \frac{1}{3700(0.02732 - x_m)} \tag{14}$$

PRV and Network

The test system can be represented by a fixed pressure supply, two gate valves, one PRV, and four pipes. The elements are arranged in series (Fig. 2), with an open pipe at the opposite end of the system to the fixed pressure. A rigid column model is sufficient to accurately represent the dynamics of the test rig (since the pipes are short). Work on the transient behavior of networks influenced by PRVs is ongoing and is the subject of a future paper. The pipes are given by

$$\dot{q} = \frac{gA}{L}\left(h_{\text{in}} - h_{\text{out}} - f_{\text{DW}}\frac{L}{D}\frac{v^2}{2g}\right) \tag{15}$$

where all the symbols have their usual meaning and $f_{\text{DW}} = 0.02$. The pipe parameters are given in Table 1. The gate valves are also described by standard equations

$$q = Ca\sqrt{|\Delta h|}\,\text{sgn}(\Delta h) \tag{16}$$

where a = cross-sectional area and C = opening. In the simulations, the area of both valves is taken as 0.007854 m^2 corre-

Table 1. Test System Pipe Dimensions

Pipe number	Length (m)	Diameter (m)
1	1.5	0.05
2	4	0.1
3	5	0.1
4	6.6	0.1

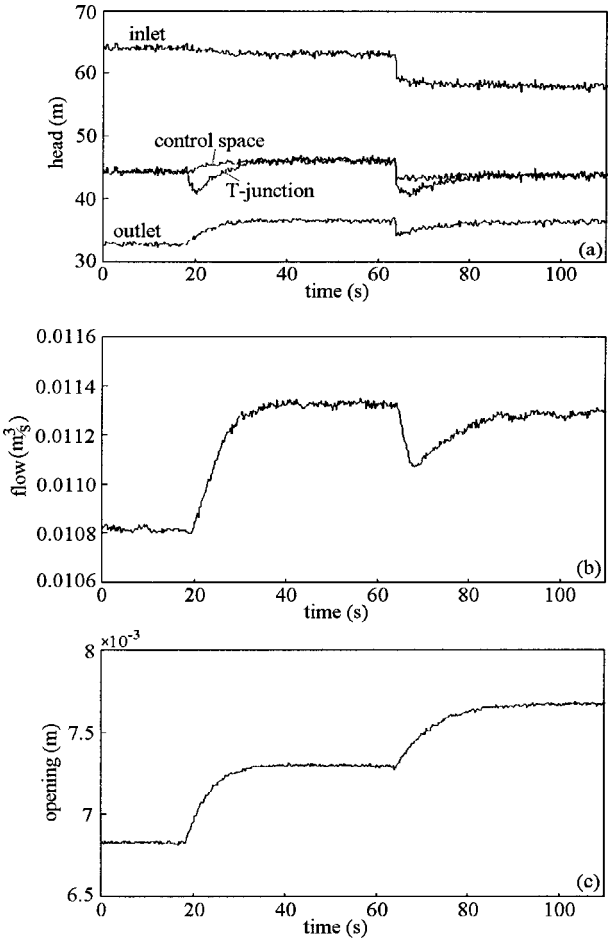

Fig. 9. Test rig measurements, Example 1—increase in set point followed by partial closure of upstream gate valve. Variables shown are inlet, outlet, T-junction, and control space pressures (a), flow through main valve (b), and the opening of main valve (c).

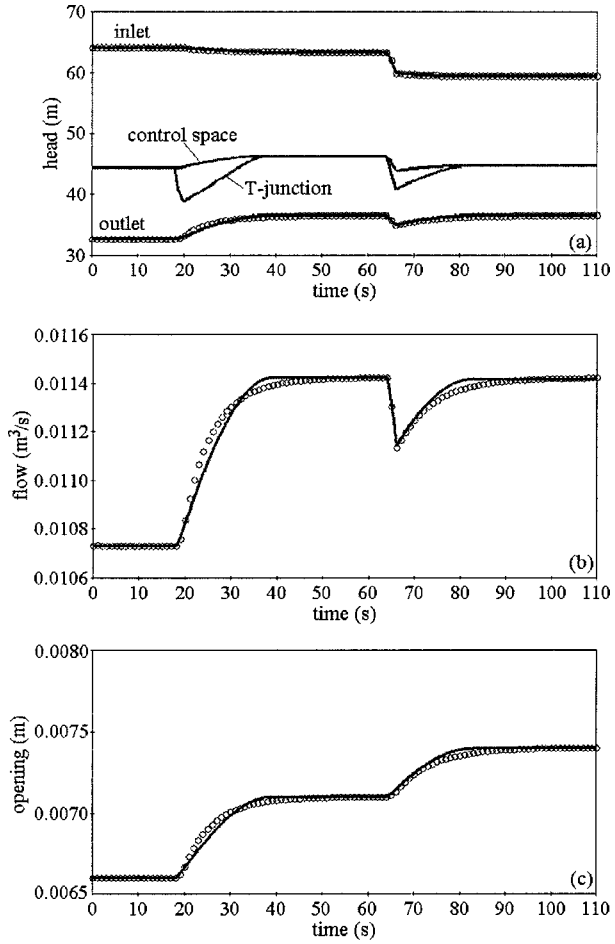

Fig. 10. Simulation results from both phenomenological models (line) and behavioral model (circles), Example 1—increase in set point followed by partial closure of upstream gate valve. Variables shown are inlet and outlet pressures (a), flow through main valve (b), and opening of main valve (c).

sponding to a diameter of 0.1 m. The components are linked by the usual head equality and flow continuity equations with a small pressure dependent leakage term. This leakage term reduces the index of the DAE system making solution easier (Brenan et al. 1996).

Model Results and Measurements

All simulations were carried out using the *gPROMS* modeling package (Process Systems Enterprise Ltd. 1997–2003). This package enables the user to solve systems comprising of interconnected components, e.g., valves and pipes. The software uses a predictor-corrector method (Gear 1971) to solve the system of equations. Experiments were carried out on the test rig shown in Fig. 2 by changing upstream and downstream valves, and the set point. These were performed for different needle valve settings. Three sets of results will be shown and simulated.

The first set of results show measurements and simulations for an increase in PRV set point followed by a partial closure of the upstream valve. In Fig. 9(a), the inlet and outlet PRV pressures and control space and T-junction pressures are shown. Figs. 9(b and c) show the main valve flow and main valve opening.

The control space and T-junction pressures are equal when the PRV reaches a steady state. The increase in set point results in the PRV opening and an increase in flow. The decrease in inlet pressure (from closing the upstream gate valve) causes the PRV to open further to maintain the outlet pressure. Following any change, the T-junction pressure drops quickly and the PRV begins to open at a speed governed by the needle valve setting.

Figs. 10(a–c) are the results of simulating the phenomenological models (lines) and the behavioral model (circles) with the downstream gate valve opening at $C=0.056$. The results from the phenomenological models are indistinguishable. The needle valve/speed control settings in the models were $C_{\text{vnv}}=0.21\times10^{-6}$ (phenomenological) and $\alpha_{\text{open}}=20\times10^{-6}$ (behavioral) resulting in a time of about 16 seconds to settle to a new steady state. Between 18 and 20 seconds the set point was changed linearly: $p_{\text{sp}}=0.0096-0.0107$ (phenomenological) and $h_{\text{set}}=32.639-36.5963$ m (behavioral). Between 64 and 66 seconds, the upstream gate valve setting was changed from $C=0.147$ to 0.11. For the phenomenological models, changing this upstream gate valve results in a change of steady state outlet pressure from 36.5963 to 36.5578 m.

Comparing Figs. 9 and 10, there is a close similarity between the simulation results and the recorded data. The opening of the PRV is approximately 0.2 mm less during the simulation than during measurements but the pressures and the flow closely match the real data. Note that the control space pressure and T-junction pressure are not available from the behavioral model.

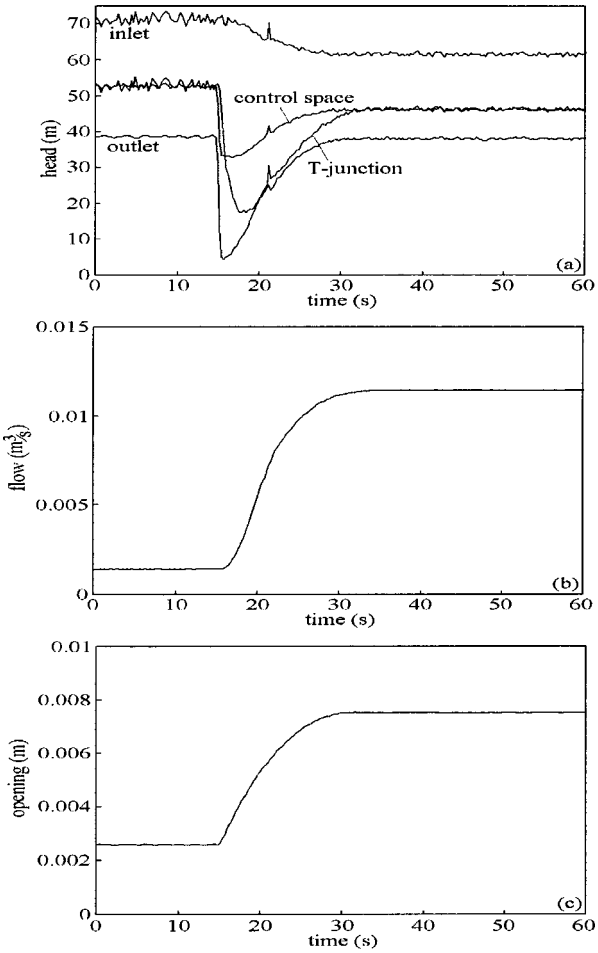

Fig. 11. Test rig measurements, Example 2—sharp opening of downstream gate valve. Variables shown are inlet, outlet, T-junction, and control space pressures (a), flow through main valve (b), and opening of the main valve (c).

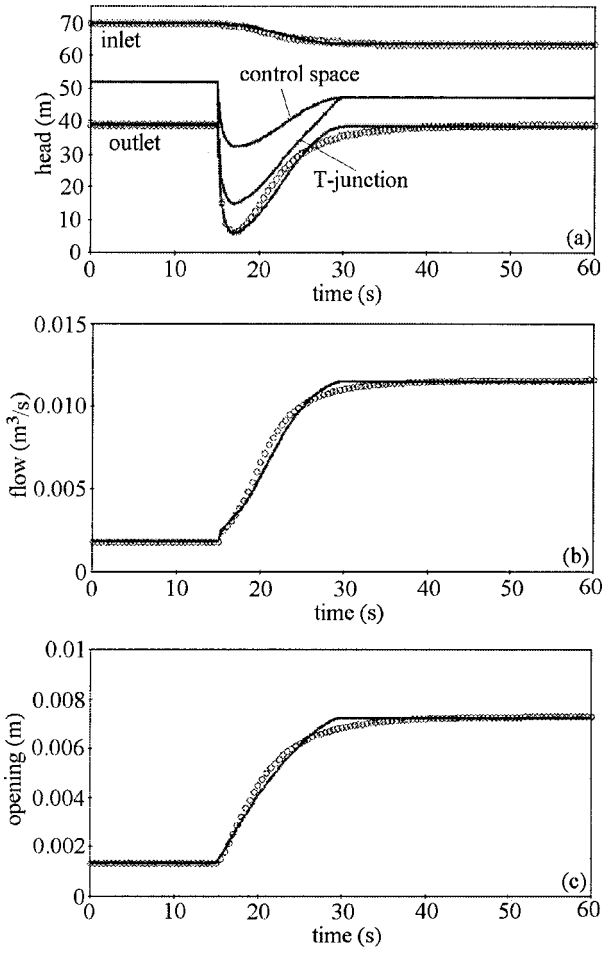

Fig. 12. Simulation results from simplified phenomenological model (line) and behavioral model (circles), Example 2—sharp opening of downstream gate valve. Variables shown are inlet and outlet pressures (a), flow through the main valve (b), and opening of main valve (c). T-junction and control space pressures for simplified model are also shown in (a).

The second set of measurements, shown in Fig. 11, display the same variables but for a change in the downstream valve setting. This valve was opened significantly from an almost closed position. The needle valve was also opened further prior to this change. This dramatic event is clearly reflected in the large changes in all the measured variables before the system settles down to a steady state once more. Such was the magnitude of the change, the simulator had difficulty solving the full phenomenological model throughout this phase.

The simplifications made to the full model to obtain the simplified model were sufficient to enable trouble-free solution. The six variables are shown as solid lines in Fig. 12. The behavioral model results are also shown (circles). Throughout this simulation, the upstream valve setting, $C=0.15$ and for the downstream valve, the setting was changed linearly from $C=0.008$ to 0.055 over two seconds. The other model parameters were $C_{\text{vnv}}=1.5\times10^{-6}$, $p_{\text{sp}}=0.0112$ (phenomenological), and $\alpha_{\text{open}}=25\times10^{-6}$, $h_{\text{set}}=38.81$ m (behavioral). The change in the needle valve setting was reflected in a slightly shorter settling time of around 13 seconds. For the phenomenological models, the steady state outlet pressure changed from 38.81 to 38.4 m.

Once again, the similarities between the simplified model and the measurements are remarkable. The only inaccurate quantity is the main valve opening during the initial phase which is attributed to a poor fit to the main valve capacity around this region (see Fig. 2).

The final set of measurements, Figs. 13(a–c), show the same quantities as the previous examples but for a decrease in PRV set point over approximately one second. The response of the PRV is faster since the needle valve presents less restriction when the flow is going into the control space (PRV closing). Once again, the fast response caused problems for simulation of the full phenomenological model.

Figs. 14(a–c) show the simulations for the simplified phenomenological model (solid lines) and the behavioral model (circles). The upstream and downstream gate valve settings were $C=0.147$ and $C=0.56$, respectively. The other model parameters were $C_{\text{vnv}}=0.00011$ (phenomenological) and $\alpha_{\text{close}}=0.0007$ (behavioral). The set point was changed over one second: $p_{\text{sp}}=0.0087-0.0078$ (phenomenological), $h_{\text{set}}=29.4-26.15$ m (behavioral). For this case, with the PRV closing, the system reached a steady state in around seven seconds.

In all measurements, minor differences can be observed between the behavioral model and the phenomenological models. In the phenomenological models, the outlet pressure is selected by adjusting the pilot valve screw which leads to small changes of

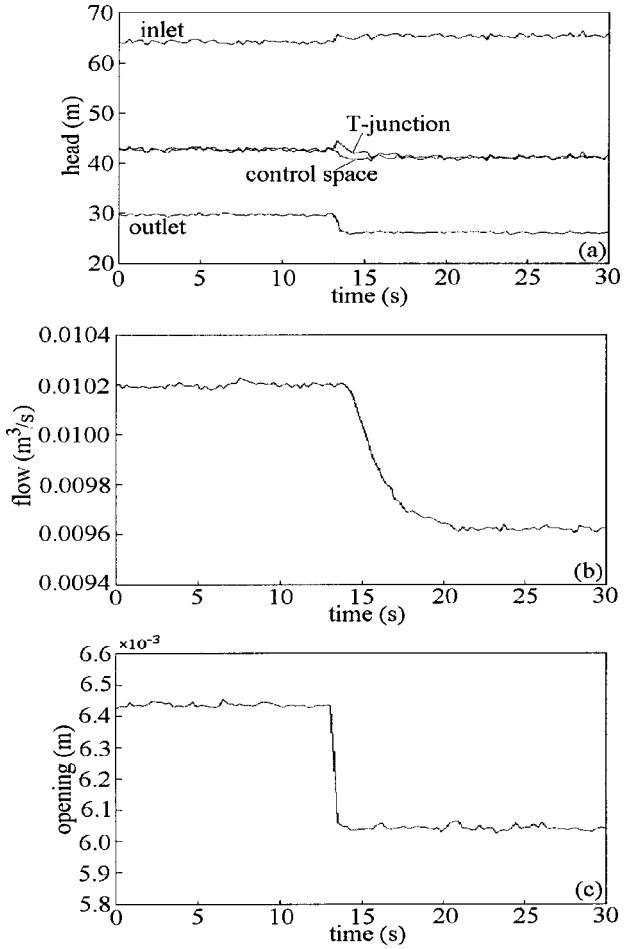

Fig. 13. Test rig measurements, Example 3—decrease of PRV set point. Variables shown are inlet, outlet, T-junction, and control space pressures (a), flow through main valve (b) and opening of main valve (c).

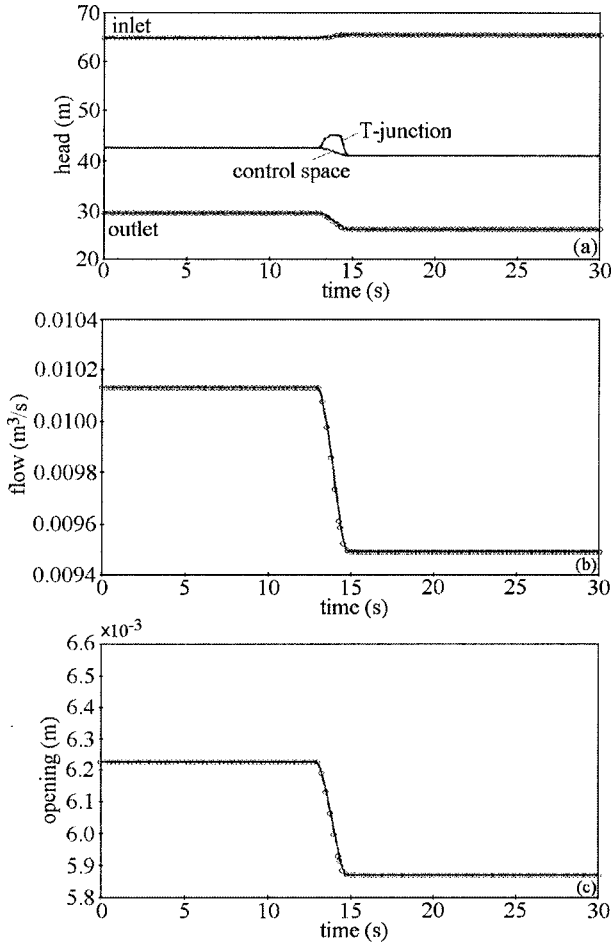

Fig. 14. Simulation results from simplified phenomenological model (line) and behavioral model (circles), Example 3—decrease of PRV set point. Variables shown are inlet, outlet, T-junction, and control space pressures (a), flow through main valve (b) and opening of main valve (c).

PRV steady state outlet pressure for changes in the system. In the behavioral model, the steady state outlet pressure is directly specified. From the model simulation results the shape of the response curve is different since the behavioral model has an exponential response and the more complex models have different nonlinearities. Although the behavioral model has fewer parameters, the main valve speed α_{open} and α_{close} have to be determined through an experimental identification procedure.

Conclusions

The dynamics of a PRV in a test rig has been investigated and dynamic models derived for use in network simulation. Two phenomenological models, closely related in structure to a PRV, have been validated under normal operating conditions and allow the behavior of PRV components to be observed. A simpler behavioral model performs similarly to the phenomenological models under the same normal operating conditions and provides an attractive option for ease of simulation. The set point of the behavioral model is given by specifying a desired outlet pressure so, in steady state, the outlet pressure will be this value. In the phenomenological models, the set point is given by the position of the pilot screw and the actual steady state outlet pressure will change a little for different inlet pressure and flow. For a given application, the choice of model will be dependent on required accuracy, network complexity, and range of operation.

A linear model of the PRV and test system has been formulated by linearizing the full phenomenological model about its steady state but is unsuitable for representing PRV dynamics since its behavior is unaffected by the needle valve setting (the fundamental mechanism which practitioners use to stabilize PRVs).

The status of a PRV is affected by its inlet and outlet pressure, the set point, and the flow through it. Since most of these are determined by the interaction between the PRV and network in which it is installed, it is inappropriate to model the PRV without taking the connected network into consideration. The combination of PRV and network also determines the speed at which the whole system will react to changes—the needle valve setting on the PRV is the principal device with which speed can be adjusted but the system will also be quicker to respond in low flow conditions and slower during periods of high flow. In the test rig experiments, the system took between 7 and 16 seconds to settle to a steady state.

Acknowledgments

This work was supported by the EPSRC, Grant No. GR/M67360. The writers would also like to thank Aztec Engineering for pro-

viding the test PRV, Hugo van Buel of Cla-val (Switzerland) for permission to use Cla-val data, Fluid Controls (UK) Ltd. for use of their test facility and John H. May for numerous enlightening discussions.

Notation

The following symbols are used in this paper:

A = cross-sectional area of pipe;
a = cross-sectional area of orifice;
a_d = area of PRV pilot valve diaphragm;
a_1 = area of PRV main valve seat;
a_2 = area of top of PRV main valve;
C = gate valve opening;
C_v = valve capacity;
C_{vfo} = valve capacity of fixed orifice;
C_{vm} = valve capacity of main valve;
C_{vnv} = valve capacity of needle valve;
C_{vp} = valve capacity of pilot valve;
c = discharge coefficient;
D = diameter of pipe;
f_{DW} = Darcy Wiesbach friction factor;
f_m = friction constant relating to main valve element;
f_p = friction constant relating to pilot valve element;
g = acceleration due to gravity;
h_c = PRV control space pressure;
h_{in} = PRV inlet pressure;
h_{out} = PRV outlet pressure;
h_{set} = PRV set point;
h_t = PRV T-junction pressure;
k_{spr} = PRV pilot spring constant;
L = length of pipe;
m_m = mass of PRV main valve element;
m_p = mass of PRV pilot valve element;
p_{sp} = representation of PRV set point;
q = flow;
q_m = flow through PRV main valve;
q_1 = flow through PRV fixed orifice;
q_2 = flow through PRV pilot valve;
q_3 = flow through PRV needle valve;
$\mathbf{u}$ = vector of control variables;
V = control space volume;
v = velocity of water in pipe;
$\mathbf{x}$ = vector of differential variables;
x_m = opening of PRV main valve element;
x_p = opening of PRV pilot valve element;
$\mathbf{y}$ = vector of algebraic variables;
α_{close} = constant representing setting of needle valve for main valve closing;
α_{open} = constant representing setting of needle valve for main valve opening;
Δh = pressure drop; and
ρ = density of water.

References

Andersen, J. H., and Powell, R. S. (1999). ''Simulation of water networks containing controlling elements.'' *J. Water Resour. Plan. Manage.*, 125(3), 162–169.

Brenan, K. E., Campbell, S. L., and Petzold, L. R. (1996). *Numerical solution of initial-value problems in differential-algebraic equation*, SIAM, Philadelphia.

Brunone, B., and Morelli, L. (1999). ''Automatic control valve-induced transients in operative pipe system.'' *J. Hydraul. Eng.*, 125(5), 534–542.

Gear, C. W. (1971). ''Simultaneous numerical solution of differential-algebraic equations.'' *IEEE Trans. Circuit Theory*, CT-18, 89–95.

Jeppson, R. W. (1976). *Analysis of flow in pipe networks*, Ann Arbor Science, Mich.

Khezzar, L., Harous, S., and Benayoune, M. (1999). ''Modeling of pressure reducing valves revisited.'' *Proc., 26th Annual Water Resource Planning and Management Conf., Preparing for the 21st Century* (CD-ROM), ASCE, Reston, Va.

McInnis, D. A., Karney, B. W., and Axworthy, D. H. (1997). ''Efficient valve representation in fixed-grid characteristics method.'' *J. Hydraul. Eng.*, 123(8), 709–718.

Prescott, S. L., and Ulanicki, B. (2001). ''Modelling the dynamic behaviour of pressure reducing valves.'' *Proc. Int. Conf. Computing and Control for the Water Industry*, Research Studies Press Ltd., Hertfordshire, England.

Press, W. H., Teukolsky, S. A., Vetterling, W. T., and Flannery, B. P. (1992). *Numerical recipes in C—the art of scientific computing*, 2nd Ed., Cambridge University Press, Cambridge, England.

Process Systems Enterprise Ltd. (1997–2003). ''*PSE:gPROMS* overview.'' ⟨http://www.psenterprise.com/products_gproms.html⟩ (April 4, 2003).

Simpson, A. R. (1999). ''Modeling of pressure regulating devices—The last major problem to be solved in hydraulic simulation.'' *Proc., 26th Annual Water Resource Planning and Management Conf., Preparing for the 21st Century*, (CD-ROM), ASCE, Reston, Va.

Streeter, V. L., Wylie, E. B., and Bedford, K. W. (1998). *Fluid mechanics*, 9th Ed., McGraw-Hill, New York.